Water Resources Research

Supporting Information for

Determining the Relative Contribution of Runoff and Coastal Processes to Compound Flood Exposure across the Carolinas during Hurricane Florence

L. E. Grimley[1], A. Sebastian[1], T. Leijnse[2,3], D. Eilander[2,4], J. Ratcliff[1,5], and R. Luettich[1,5]

[1]Department of Earth, Marine and Environmental Sciences, University of North Carolina at Chapel Hill, Chapel Hill, NC, USA, [2]Institute for Environmental Studies (IVM), Vrije Universiteit Amsterdam, Amsterdam, the Netherlands, [3]Department of Marine and Coastal Systems, Deltares, Delft, the Netherlands, [4]Department of Inland and Water Systems, Deltares, Delft, the Netherlands, [5]UNC Institute of Marine Sciences, Morehead City, NC, USA.

Contents of this file

Text S1 to S3
Figures S1 to S13
Tables S1 to S7

Introduction

The supporting information provides additional detail on the model setup, boundary conditions, and sensitivity analysis (Section 1). Supplementary figures are provided to complement the figures in the results section of the main text (Section 2). Additional figures show the results of the model performance compared to observation data collected at USGS gages and high-water marks (HWM) from Hurricane Matthew (2016) (Section 3).

S1. Model Setup, Boundary Conditions, and Sensitivity Analysis

In this section, additional detail on the SFINCS model setup including waterbody delineation, channel bathymetry, and Manning's n values is provided. We also provide details of the water level, discharge, rainfall, and wind inputs for Hurricane Florence and tables on the results of sensitivity runs demonstrating how model skill score varies according to model inputs.

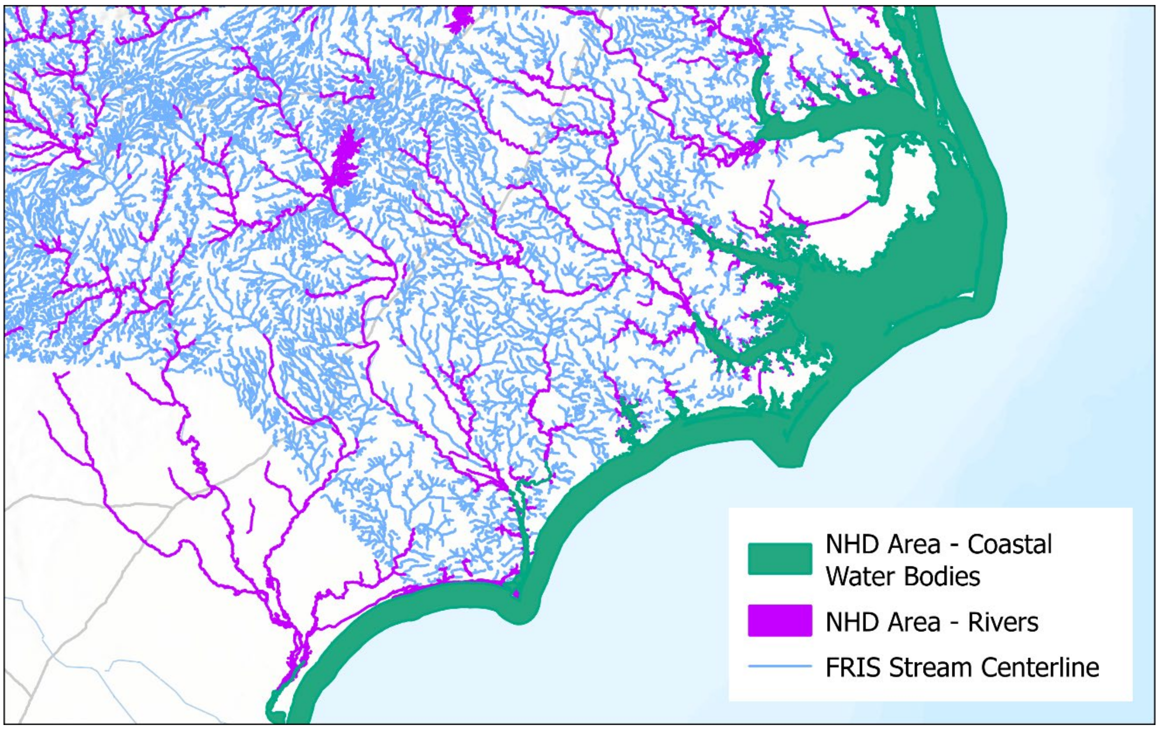

Figure S1. Water masks were used to assign boundary cells in SFINCS, add bathymetry, and update the Manning's roughness. Water masks that were used include the NHD Area shapefile (purple) which was modified to improve the delineation of the estuaries and sounds for a coastal water body mask (green), and the North Carolina (NC) Flood Risk Information System (FRIS) stream centerline (blue) which was used to identify smaller streams as the NHD Flowline dataset was incomplete with discontinuities.

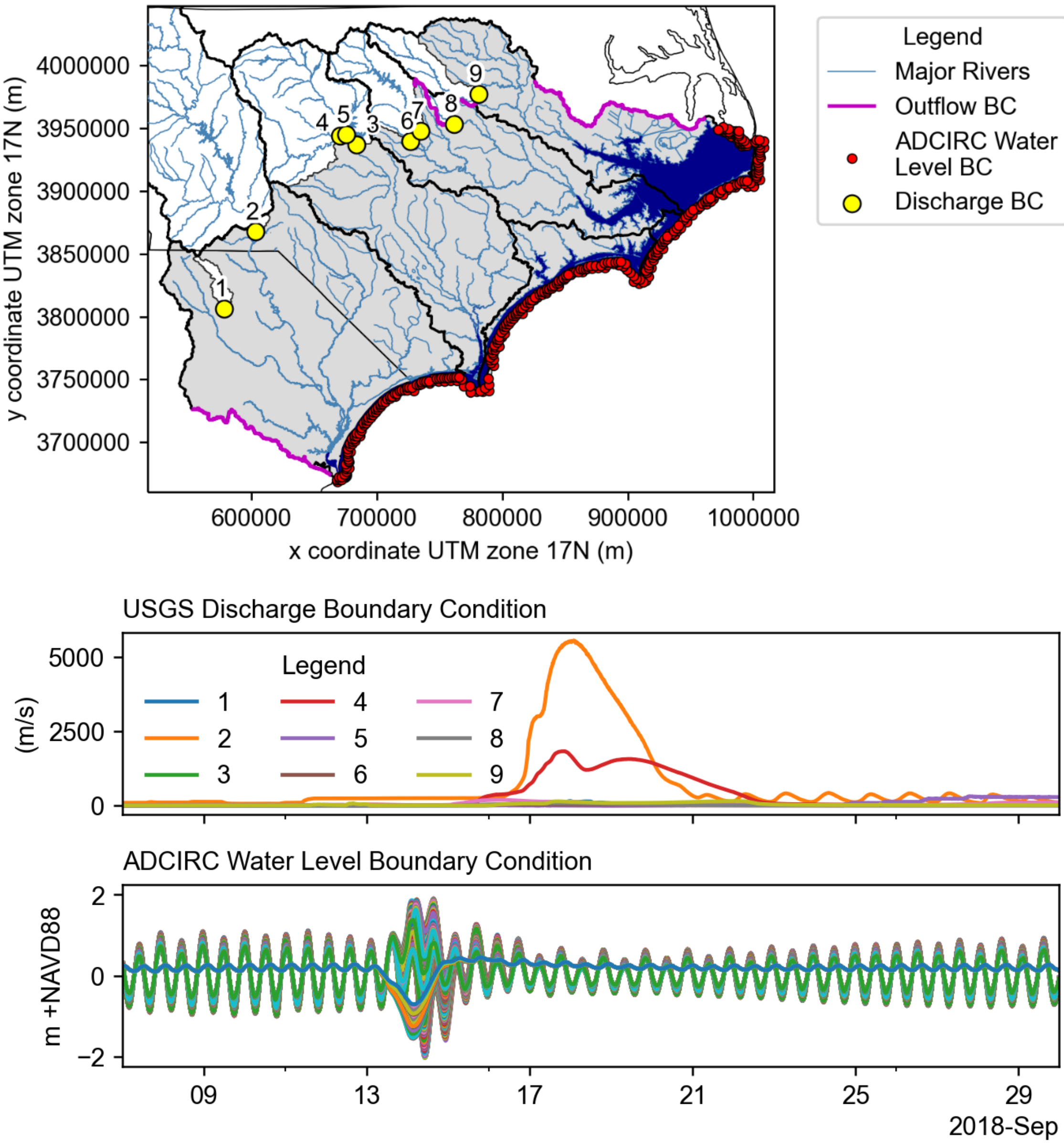

Figure S2. The top panel shows the study area included in the model (grey) and the boundary conditions including 9 USGS discharge inputs (green dots), 341 ADCIRC water levels applied to the downstream water level boundary (red dots), and outflow boundaries (purple) where flow can exit the domain. The middle panel shows the time series of discharge (m/s) on a log scale where the streamflow inputs to the Lower Pee Dee (Pt 1) and Cape Fear (Pt 2) basins are the greatest. The bottom panel shows the time series of 341 ADCIRC water levels (m +NAVD88) interpolated to the SFINCS coastal boundary.

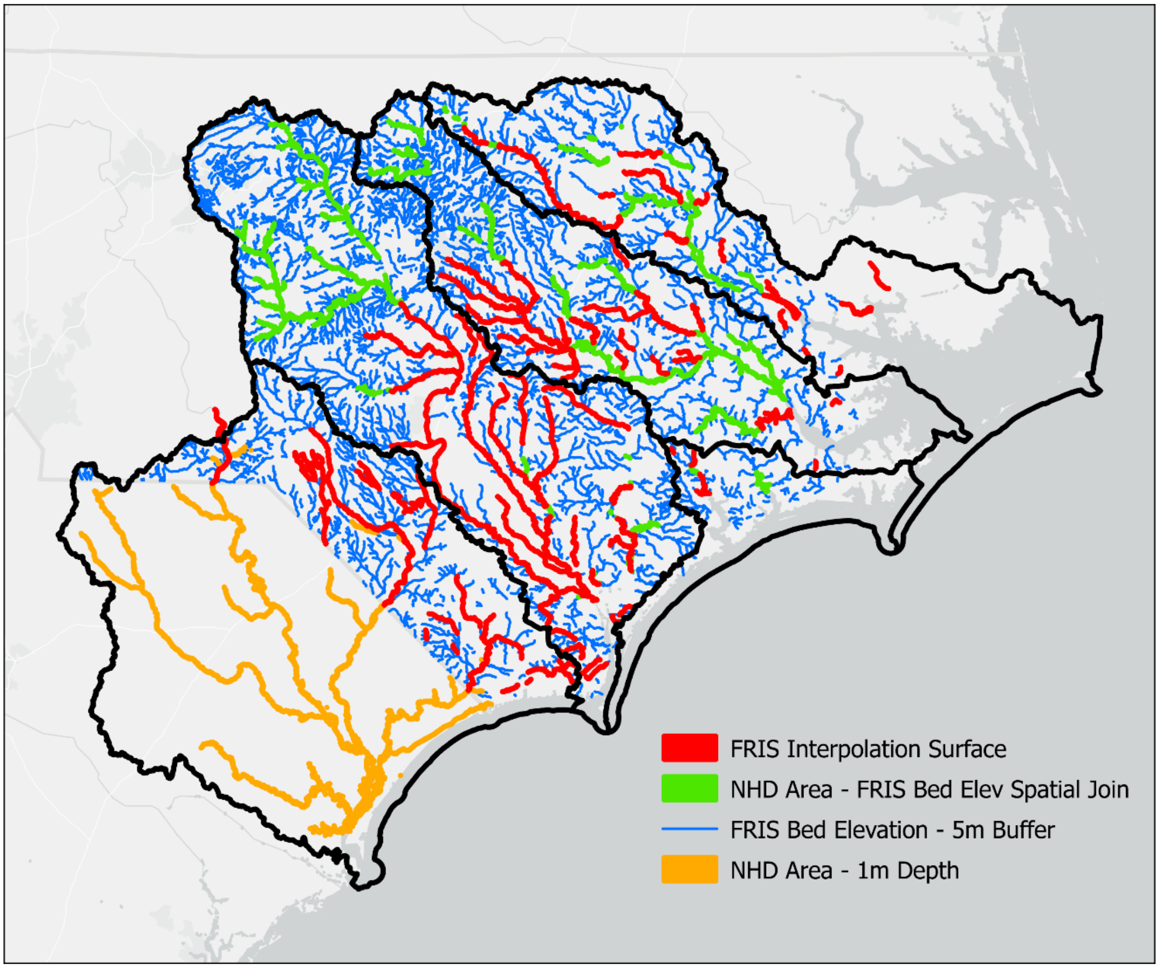

Figure S3. Rivers and streams were burned into the DEM prior to assigning grid and subgrid elevations. The most detailed bathymetric data was sourced by interpolating cross-section survey data obtained from the HEC-RAS 1D river models available from NC FRIS (red). Where interpolated surfaces were not available, the maximum depth recorded in the HEC-RAS 1D cross-sections was linearly interpolated onto a 5.0 m raster masked by the NHD Area polygon shapefile (green). For smaller tributary streams, stream centerlines of the HEC-RAS 1D river models (blue) were used to assign the maximum depth of the channel from the cross-sectional data. The values were then assigned to a 5.0 m raster using the nearest point. Detailed data was not available for South Carolina (SC); instead, in SC, we subtracted 2.0 m from the DEM for the NHD Areas (orange).

Table S1. Ranges of common Manning's roughness coefficients for Multi-resolution Land Characteristics (MLRC) Consortium's National Land Cover Dataset (NLCD). We apply the average values to the SFINCS model. We used the NHD Area to assign Manning's n for large rivers and a modified version of this shapefile clipped to the estuaries and coastlines to assign Manning's n to open water bodies (Dietrich et al., 2010). For smaller streams that are not in the NHD Area shapefile, we use the NC FRIS stream centerline to assign Manning's n for smaller rivers where dense vegetation and wood debris can impede flow in the channel (Liu et al., 2019; Savage et al., 2016).

Land Cover Type	Low	Average	High
open water	0.020	0.023	0.025
perennial snow/ice	0.020	0.022	0.024
developed, open space	0.030	0.040	0.050
developed, low intensity	0.080	0.100	0.120
developed, medium intensity	0.060	0.100	0.140
developed, high intensity	0.120	0.160	0.200
barren land	0.023	0.027	0.030
deciduous forest	0.100	0.130	0.160
evergreen forest	0.100	0.130	0.160
mixed forest	0.100	0.130	0.160
shrub/scrub	0.070	0.115	0.160
herbaceous	0.025	0.038	0.050
hay/pasture	0.025	0.038	0.050
cultivated crops	0.025	0.038	0.050
woody wetlands	0.070	0.115	0.160
emergent herbaceous wetlands	0.070	0.115	0.160
large rivers (>30m width)	0.025	0.030	0.045
smaller rivers/streams (<30m width)	0.035	0.045	0.055

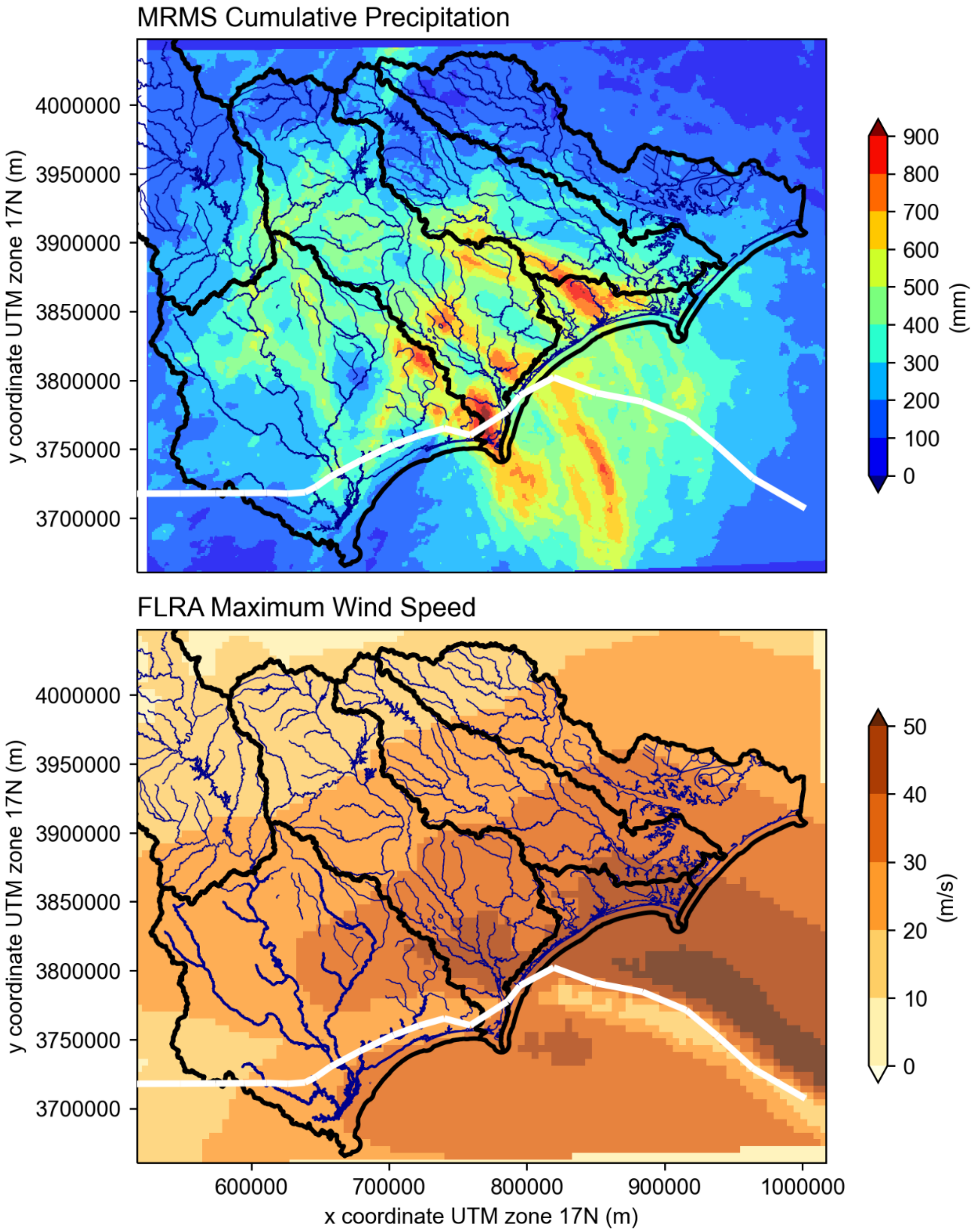

Figure S4. The top panel shows the total precipitation (mm) from the MRMS radar-rainfall dataset applied to the model domain for the 23-day simulation of Hurricane Florence. The bottom panel shows the max wind speed (m/s) of the FLRA dataset calculated using the 11 days the data was available.

Table S2. Sensitivity analysis of model skill for SFINCS grid resolution, Manning's roughness, and channels. The Lower Pee Dee (LPD) HUC6 basin has a constant depth subtracted from the DEM whereas all other channels were defined using HEC-RAS data. All models use a 5m subgrid resolution. The difference in skill relative to the base scenario (bolded) is shown.

Model			Water Level Gages				HWMs	
Grid (m)	Manning's N	Channels	PE (m)	Bias (m)	RMSE (m)	R-squared	Bias (m)	RMSE (m)
200	**Average**	**Yes, LPD 2m**	**0.33**	**-0.29**	**1.35**	**0.56**	**0.05**	**0.93**
200	Average	Yes, LPD 1m	0.06	0.10	-0.01	0.00	0.04	0.04
100	Average	Yes, LPD 1m	0.22	0.22	-0.03	0.00	0.18	0.02
200	High	Yes, LPD 2m	0.12	0.17	-0.15	0.12	0.09	0.00
200	Low	Yes, LPD 2m	-0.17	-0.21	0.18	-0.12	-0.14	0.02
200	Average	No	0.30	0.71	-0.14	-0.01	0.20	0.12

Table S3. Sensitivity analysis of model skill of the Lower Pee Dee HUC6 basin for Manning's roughness and channel depths. All models use a 5m subgrid resolution. The difference in skill relative to the base scenario (bolded) is shown.

Model			Water Level Gages				HWMs	
Grid (m)	Manning's N	Channels	PE (m)	Bias (m)	RMSE (m)	R-squared	Bias (m)	RMSE (m)
200	**Average**	**2m**	**0.65**	**0.06**	**1.24**	**0.43**	**0.42**	**0.84**
200	Average	1m	0.00	0.21	-0.03	0.13	0.09	0.10
100	Average	1m	0.00	0.26	0.03	0.26	0.19	0.15
200	Average	No	-0.03	0.44	-0.02	0.25	0.21	0.20

S2. Hurricane Florence Results

In this section, we provide additional tables and figures showing the modeled water surface elevations compared against observed water level records from Hurricane Florence. A map of the maximum flood depths simulated by the model and additional figures of forcing attribution are also provided.

Table S4. Modeled water levels were compared against 89 water level gages (76 USGS, 5 NOAA, 7 USGS Rapid Deployment (RD), 1 NCEM) using statistics of the Peak Error, Bias, Root-Mean-Square-Error (RMSE), and Coefficient of Determination (R-squared) which were calculated across the 23-day simulation.

Agency	Site ID	RMSE (m)	Bias (m)	R-Squared	Peak Error (m)	HUC6 Watershed
USGS	210869230	0.85	0.13	0.41	1.38	Cape Fear
USGS	2105769	2.65	-2.22	0.79	-0.49	Cape Fear
USGS	2108566	1.06	-0.60	0.90	-0.08	Cape Fear
USGS	2106500	3.10	-2.19	0.34	-0.41	Cape Fear
USGS	2108000	1.03	-0.38	0.73	-0.40	Cape Fear
USGS	2105500	4.33	-2.96	0.79	0.05	Cape Fear
USGS	2104000	2.84	-1.25	0.83	0.49	Cape Fear
USGS	2102908	0.80	0.04	0.38	0.57	Cape Fear
USGS	2103000	2.96	-1.90	0.47	-0.70	Cape Fear
USGS	2102500	0.58	-0.34	0.96	0.04	Cape Fear
USGS	2104220	1.70	-1.27	0.45	1.46	Cape Fear
NOAA	8658120	0.63	0.07	0.45	0.63	Cape Fear
USGS-RD	2108619	0.73	0.60	0.85	1.73	Cape Fear
USGS-RD	2105544	5.66	-5.07	0.90	-2.11	Cape Fear
USGS	2136361	0.50	0.47	0.42	0.57	Lower Pee Dee
USGS	2135615	0.33	0.13	0.07	0.53	Lower Pee Dee
USGS	21355015	0.23	0.06	0.40	0.39	Lower Pee Dee
USGS	2135501	0.41	0.18	0.54	0.56	Lower Pee Dee
USGS	2131500	1.58	-0.40	0.18	0.38	Lower Pee Dee
USGS	2131472	1.00	0.95	0.45	0.22	Lower Pee Dee
USGS	2131455	0.97	-0.84	0.80	-0.48	Lower Pee Dee
USGS	21313485	0.64	-0.53	0.44	-0.39	Lower Pee Dee
USGS	2131452	1.12	-0.90	0.66	-0.32	Lower Pee Dee
USGS	2110815	0.76	-0.28	0.28	0.44	Lower Pee Dee
USGS	21108125	1.20	0.35	0.20	1.49	Lower Pee Dee
USGS	2110802	1.45	0.02	0.29	1.01	Lower Pee Dee
USGS	2135200	1.70	0.05	0.39	0.81	Lower Pee Dee
USGS	2110725	1.48	0.38	0.29	1.42	Lower Pee Dee
USGS	2110704	1.07	-0.24	0.69	0.47	Lower Pee Dee

USGS	2110550	1.15	-0.21	0.77	0.08	Lower Pee Dee
USGS	2110777	0.30	-0.17	0.74	-0.06	Lower Pee Dee
USGS	2110701	1.03	-0.23	0.69	0.36	Lower Pee Dee
USGS	2110500	1.26	-0.49	0.20	0.08	Lower Pee Dee
USGS	2136350	0.32	-0.12	0.68	-0.08	Lower Pee Dee
USGS	2136030	1.16	0.69	0.92	2.03	Lower Pee Dee
USGS	2136000	0.85	0.71	0.55	1.00	Lower Pee Dee
USGS	2131510	1.43	-0.50	0.02	0.47	Lower Pee Dee
USGS	2132000	2.33	0.90	0.06	1.24	Lower Pee Dee
USGS	2135000	1.21	0.09	0.30	1.14	Lower Pee Dee
USGS	2131010	1.23	-0.05	0.70	-0.11	Lower Pee Dee
USGS	2131000	1.58	0.49	0.68	-0.18	Lower Pee Dee
USGS	2130980	1.39	-0.19	0.20	0.63	Lower Pee Dee
USGS	2109500	1.37	-0.85	0.44	-0.12	Lower Pee Dee
USGS	2110400	1.20	-0.69	0.20	0.02	Lower Pee Dee
USGS	2134900	1.60	-0.11	0.17	1.30	Lower Pee Dee
USGS	2134500	1.36	-0.95	0.48	-0.04	Lower Pee Dee
USGS	2134170	1.00	-0.38	0.58	0.09	Lower Pee Dee
USGS	2134480	0.72	-0.50	0.62	0.14	Lower Pee Dee
USGS	2130810	1.86	0.82	0.68	-0.33	Lower Pee Dee
USGS	2130561	3.85	3.08	0.87	-1.09	Lower Pee Dee
USGS	2132320	0.58	-0.05	0.29	0.97	Lower Pee Dee
USGS	2133624	2.10	-1.48	0.09	0.53	Lower Pee Dee
USGS	2129375	0.41	-0.11	0.98	0.34	Lower Pee Dee
USGS	2133500	1.23	-0.77	0.49	0.93	Lower Pee Dee
NOAA	8661070	0.19	-0.06	0.91	-0.19	Lower Pee Dee
USGS-RD	2135100	2.28	1.33	0.12	2.10	Lower Pee Dee
USGS-RD	2132500	0.89	-0.44	0.68	1.02	Lower Pee Dee
USGS-RD	2130000	4.16	3.45	0.90	-0.39	Lower Pee Dee
USGS	2092554	1.65	-0.68	0.49	0.77	Neuse
USGS	2092500	2.82	-2.53	0.62	-0.76	Neuse
USGS	2092576	0.25	-0.07	0.84	-0.14	Neuse
USGS	209205053	0.70	-0.31	0.61	0.47	Neuse
USGS	2089500	2.82	-1.70	0.26	0.54	Neuse
USGS	2091814	1.97	-1.16	0.16	0.72	Neuse
USGS	2089000	2.82	-1.75	0.40	0.22	Neuse
USGS	2091500	1.97	-1.49	0.77	0.23	Neuse
USGS	2091000	0.87	-0.54	0.65	-0.07	Neuse
USGS	2088500	0.95	-0.73	0.79	-0.55	Neuse
USGS	2087570	0.48	0.08	0.89	0.25	Neuse
USGS	2088000	1.65	-1.52	0.66	-0.51	Neuse

USGS	2088383	2.43	-2.41	0.64	-1.62	Neuse
NCEM	VNCN7	0.99	-0.29	0.47	0.99	Neuse
USGS	2093222	0.37	0.04	0.54	0.00	Onslow Bay
USGS	2093206	0.31	-0.06	0.36	0.49	Onslow Bay
USGS	209270825	0.30	0.00	0.47	-0.24	Onslow Bay
USGS	2093000	2.58	-2.30	0.71	-2.24	Onslow Bay
NOAA	8658163	0.16	-0.05	0.91	0.16	Onslow Bay
NOAA	8656483	0.18	-0.12	0.90	-0.06	Onslow Bay
USGS-RD	2092712	0.34	-0.11	0.44	-0.32	Onslow Bay
USGS-RD	209303201	0.27	0.08	0.84	0.50	Onslow Bay
USGS	2084472	0.17	-0.11	0.91	0.22	Pamlico
USGS	2084160	0.48	-0.41	0.83	-0.08	Pamlico
USGS	2084557	0.96	0.94	0.69	1.23	Pamlico
USGS	2083500	2.76	2.68	0.83	2.54	Pamlico
USGS	2082585	0.68	-0.54	0.89	0.10	Pamlico
USGS	2082770	1.67	1.63	0.61	2.05	Pamlico
USGS	2083000	1.39	1.36	0.42	1.23	Pamlico
USGS	2082950	1.67	1.59	0.77	2.59	Pamlico
NOAA	8654467	0.25	-0.19	0.33	-0.25	Pamlico

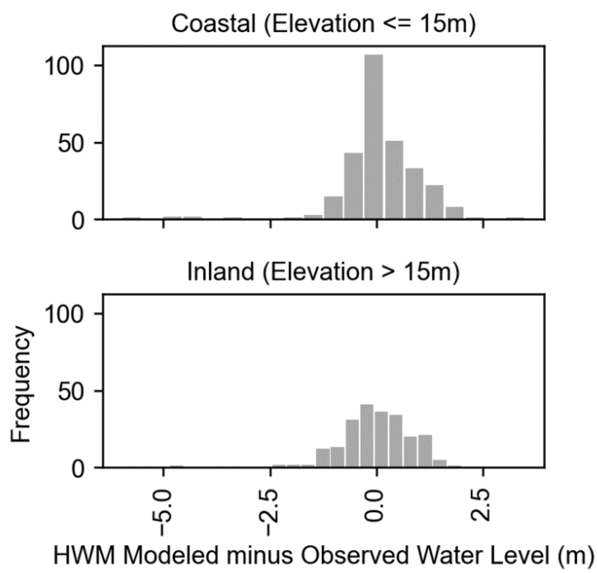

Figure S5. The difference between modeled and observed water levels for Hurricane Florence at 512 HWM locations for coastal and inland areas. The upper panel indicates that while the model performance is generally better at coastal locations, as shown by tighter distribution around 0, there are several outliers where the observed water levels are much larger (>2.5 m) than the modeled water levels.

Table S6. The average Bias (m) and RMSE (m) for each HUC6 was calculated using the modeled peak water levels compared to the observed HWMs.

HUC6 Watershed	RMSE (m)	Bias (m)
Lower Pee Dee	0.84	0.42
Neuse	0.83	-0.22
Cape Fear	1.27	-0.36
Pamlico	0.27	-0.13
Onslow Bay	0.61	-0.17

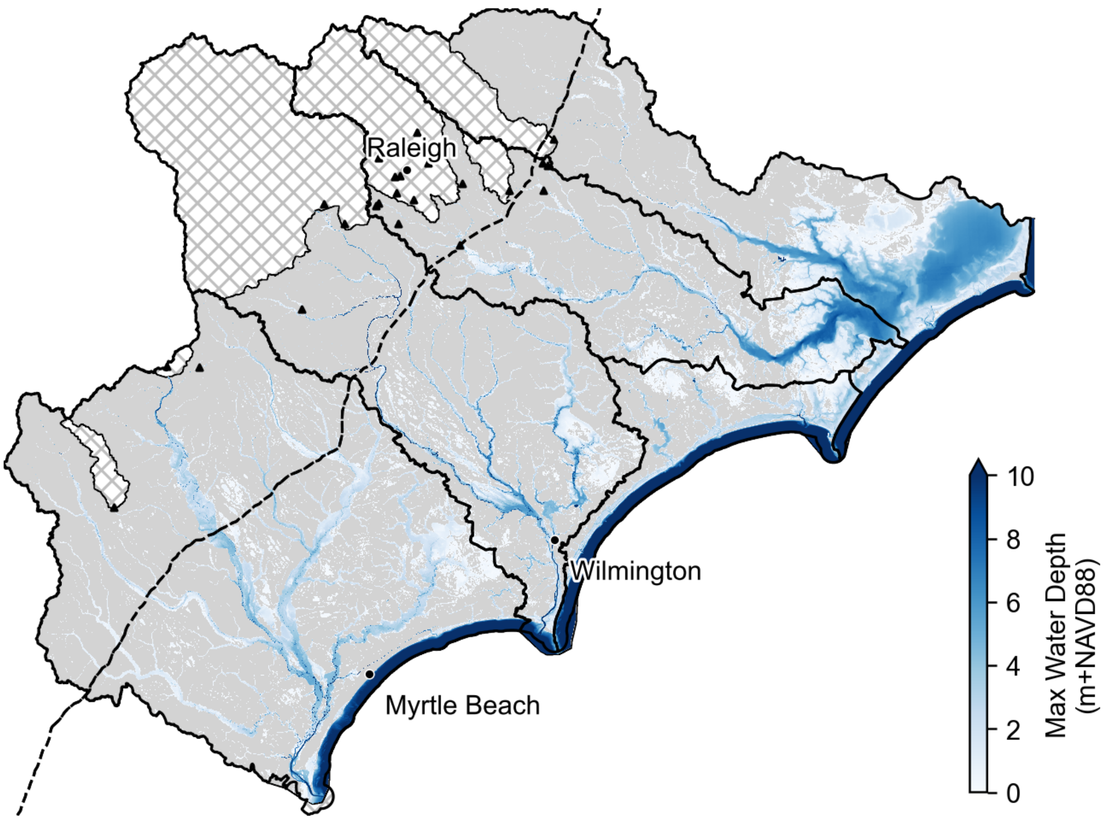

Figure S6. SFINCS modeled peak water level for the compound scenario (C+W+Q+P) for Hurricane Florence.

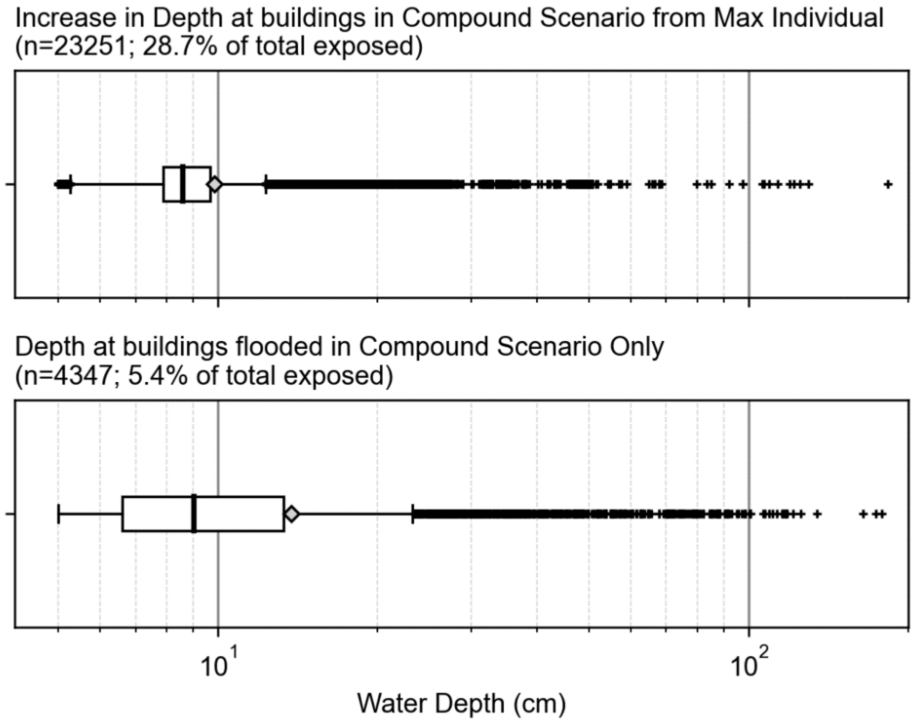

Figure S7. The top panel shows the difference in maximum depth (cm) between the compound scenario and the individual drivers (e.g., coastal, runoff). Compound flooding increases the depth at 23,251 buildings by a mean of 0.10 m. The bottom panel shows the depths at structures (n=4,347) that were only exposed to >= 0.05 m of flooding in the compound flood scenario with no exposure in the coastal or runoff scenarios. Compound flooding increases the number of buildings exposed to flooding and the mean depth. Water depth (cm) is logged on the x-axis. The median is indicated by thick black line and the mean is noted by a grey diamond. The number of buildings (n) is listed below the scenario name.

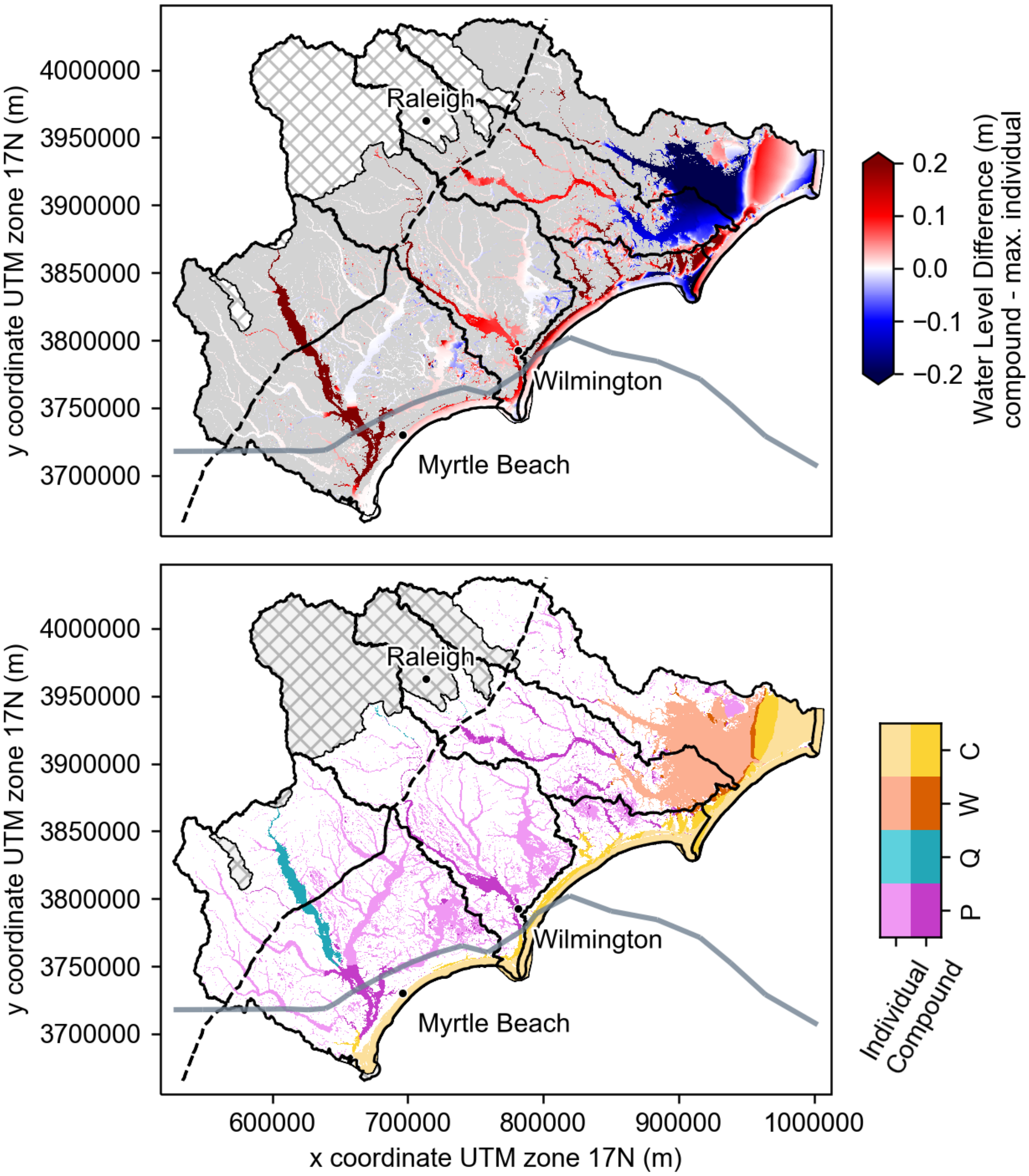

Figure S8. The top panel shows the difference in peak water level between the compound scenario (C+W+Q+P) and the largest depth from using individual forcings including coastal water level (C), wind (W), discharge (Q) and precipitation (P). The bottom panel shows the dominant drivers (i.e., coastal and runoff) which are darker for areas where the compound scenario increased total water levels by at least 0.05 m.

S3. Hurricane Matthew Boundary Conditions and Validation

In this section, we provide additional figures showing model boundary conditions (Figures S8 and S9) and validation results for Hurricane Matthew (2016). Matthew remained close to the NC coast moving slowly along a shore-parallel track (see Figure S9). We simulate 12 days of water levels across the Carolinas for Hurricane Matthew (October 3, 2016 00:00 to October 15, 2016 00:00) using USGS discharge at the upstream boundary and MRMS radar rainfall applied directly to the grid. We apply ADCIRC water levels at the coastal boundary and Ocean Weather Incorporated (OWI) winds to the grid for the first 9 days because that is when the data was available (Thomas et al., 2019).

We validated the modeled water levels against 61 USGS gages (Figure S10), reporting performance statistics by HUC6 watershed in Table S7. The model error matches the validation results of Hurricane Florence where the model bias tends to be negative (-0.73 m). However, the model shows skill in predicting peak water levels during Matthew at USGS gages with an error of 0.0 m. We compared modeled peak water levels to observations at 385 HWMs ranging between 0-50 m+NAVD88 in Figure S11, highlighting that TC flooding often occurs beyond the coastal zone (e.g., >20 m+NAVD88). The model tends to underpredict peak water levels with a bias of -0.36 m and RMSE of 0.94 m. The error is greater in the coastal zone than inland areas (Figure S12). Compared to the Florence hindcast, we used coarser ADCIRC model and unadjusted OWI winds which may explain larger errors at the coast.

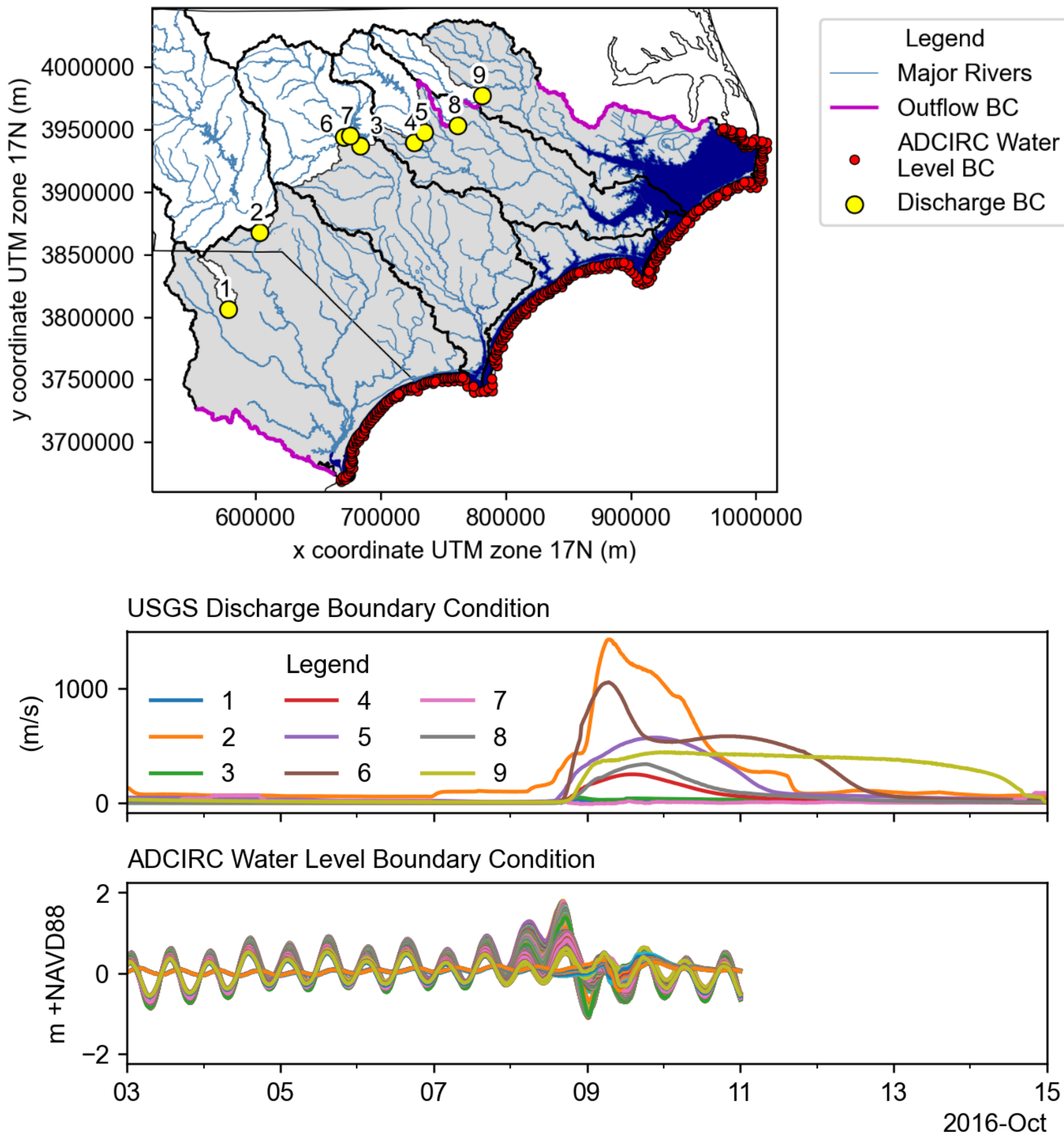

Figure S9. The top panel shows the study area included in the model (grey) and the boundary conditions including 9 USGS discharge inputs (yellow dots), 341 ADCIRC water levels applied to the downstream water level boundary (red points), and outflow boundaries (purple) where flow can exit the domain. The middle panel shows the time series of discharge (m/s) on a log scale where the streamflow inputs to the Lower Pee Dee (Pt 1) and Cape Fear (Pt 2) basins are the greatest. The bottom panel shows the timeseries of 341 ADCIRC water levels (m +NAVD88) applied to the SFINCS coastal boundary.

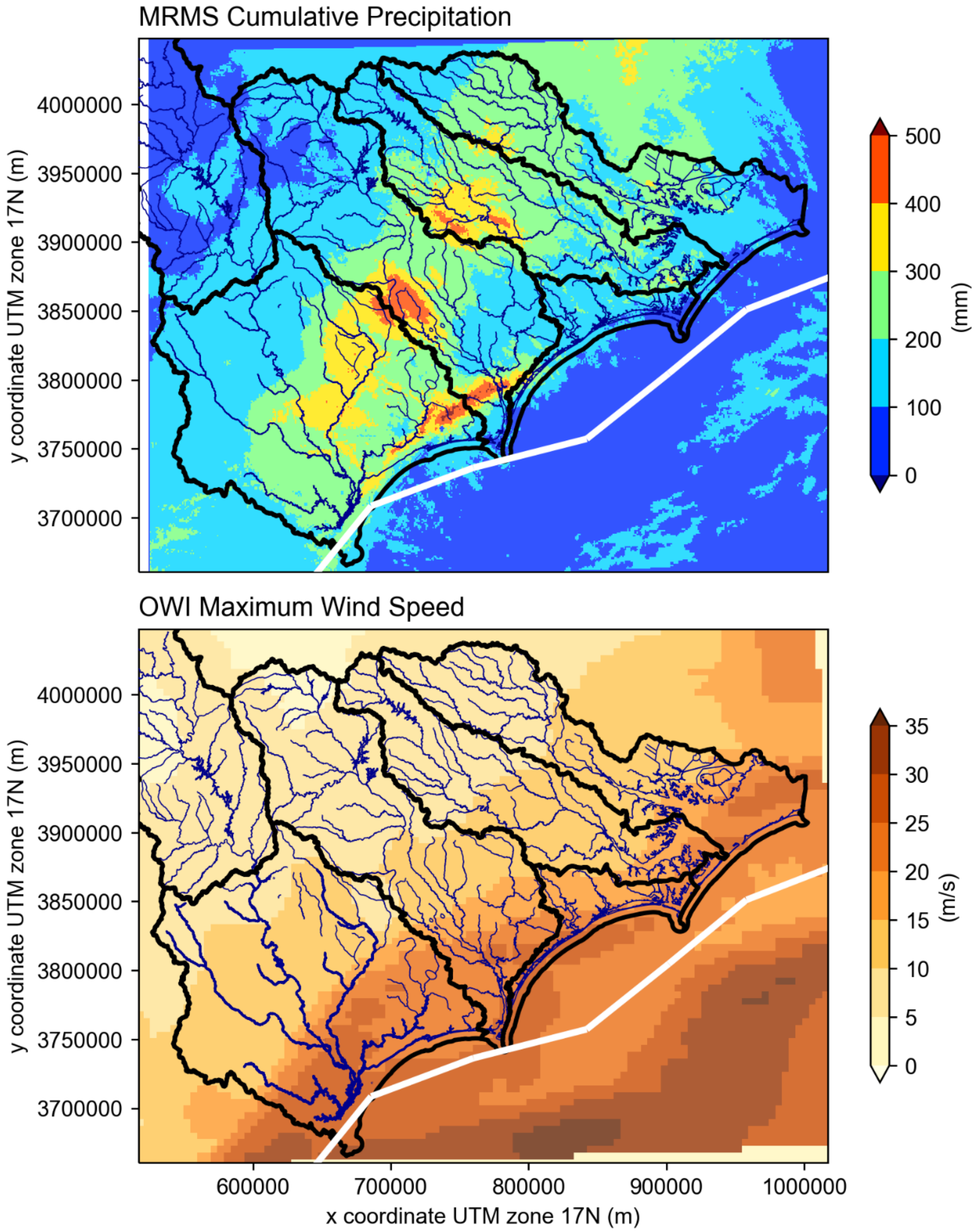

Figure S10. The top panel shows the total precipitation (mm) across the study for Hurricane Matthew (2016) using MRMS radar-rainfall. The bottom panel shows the max wind speed (m/s) of the Ocean Weather Inc. (OWI) dataset.

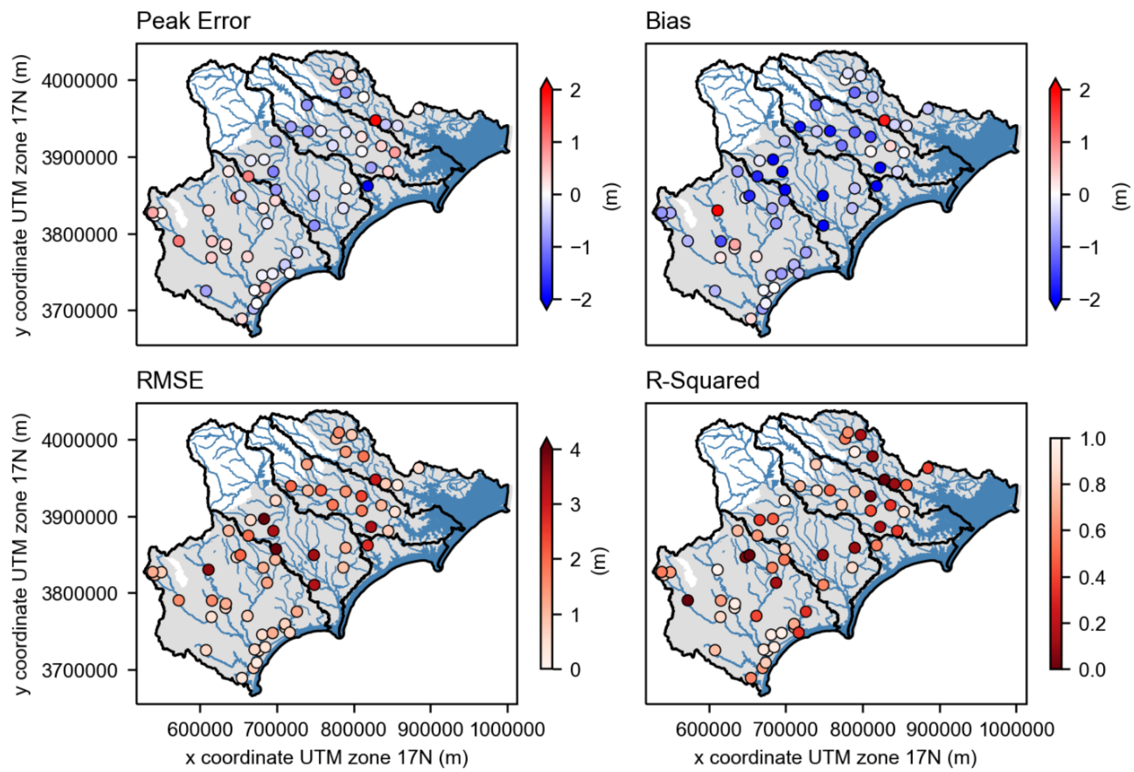

Figure S11. Peak Error (m), Bias (m), Root-Mean-Square-Error (RMSE) (m), and Coefficient of Determination (R-squared) statistics were calculated comparing SFINCS modeled water levels for Hurricane Matthew to observations at 61 USGS gages.

Table S7. Modeled water levels were compared to gage observations using statistics of the Peak Error, Bias, Root-Mean-Square-Error (RMSE), and Coefficient of Determination (R-squared) for Hurricane Matthew. These metrics were averaged across the USGS gages for each HUC6 watershed which can be compared to the values averaged across the entire domain.

HUC6 Watershed (n=USGS gages)	RMSE (m)	Bias (m)	R-Squared	Peak Error (m)
Cape Fear (n=10)	2.41	-1.88	0.58	-0.34
Lower Pee Dee (n=29)	0.97	-0.33	0.64	0.12
Neuse (n=12)	1.62	-1.01	0.55	-0.18
Onslow Bay (n=1)	2.75	-2.45	0.57	-2.91
Pamlico (n=9)	1.25	-0.15	0.37	0.57
Domain (n=61)	1.40	-0.73	0.57	0.00

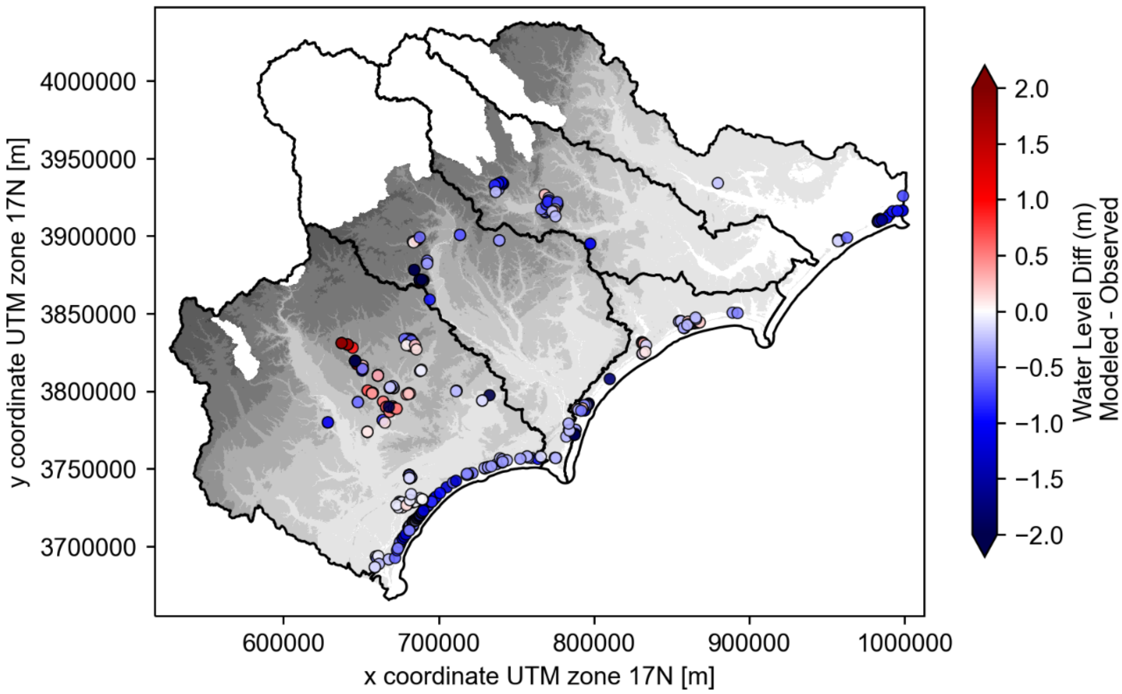

Figure S12. Modeled peak water levels for Hurricane Matthew were compared to observations of USGS high-water marks (HWMs) with a quality of 'fair' or better. The bias (m) is shown at each location.

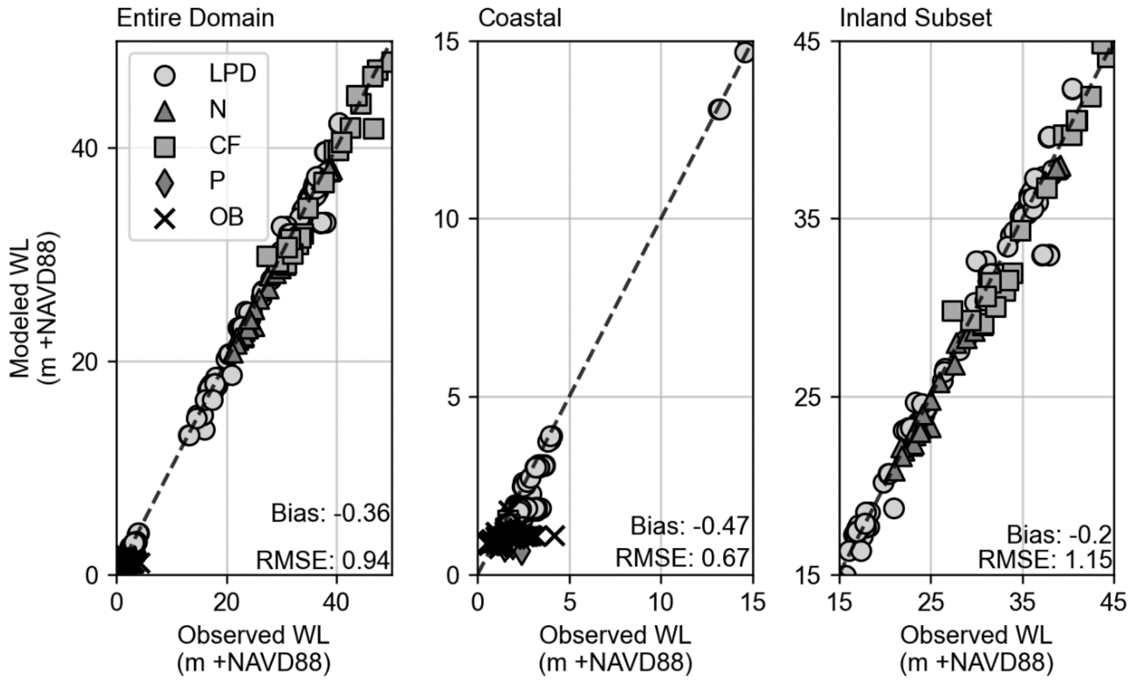

Figure S13. Observed and modeled peak water levels were compared at USGS High Water Mark (HWM) locations across the five HUC6 watersheds (Lower Pee Dee (LPD), Neuse (N), Cape Fear (CF), Pamlico (P), and Onslow Bay (OB)) for Hurricane Matthew. Note, the scale of the axis changes for each subplot and the model bias and RMSE for the data shown is listed in the bottom right corner.

References

Dietrich, J. C., Bunya, S., Westerink, J. J., Ebersole, B. A., Smith, J. M., Atkinson, J. H., et al. (2010). A High-Resolution Coupled Riverine Flow, Tide, Wind, Wind Wave, and Storm Surge Model for Southern Louisiana and Mississippi. Part II: Synoptic Description and Analysis of Hurricanes Katrina and Rita. Monthly Weather Review, 138(2), 378–404. https://doi.org/10.1175/2009MWR2907.1

Liu, Z., Merwade, V., & Jafarzadegan, K. (2019). Investigating the role of model structure and surface roughness in generating flood inundation extents using one- and two-dimensional hydraulic models. Journal of Flood Risk Management, 12(1). https://doi.org/10.1111/jfr3.12347

Savage, J. T. S., Pianosi, F., Bates, P., Freer, J., & Wagener, T. (2016). Quantifying the importance of spatial resolution and other factors through global sensitivity analysis of a flood inundation model. Water Resources Research, 52(11), 9146–9163. https://doi.org/10.1002/2015WR018198

Thomas, A., Dietrich, J., Asher, T., Bell, M., Blanton, B., Copeland, J., et al. (2019). Influence of storm timing and forward speed on tides and storm surge during Hurricane Matthew. Ocean Modelling, 137, 1–19. https://doi.org/10.1016/j.ocemod.2019.03.004